Spin-valley coupling in MoS_2

The goal of this document is to understand the basic physics of spin-valley coupling in MoS_2. To get there, we need to start with some fundamentals. We will begin with a generic discussion of adiabatic processes and Berry phase, which will then be applied towards understanding what the Berry phase has to do with solid state physics. From this basic understanding, we can tackle the problem of MoS_2.

1 Adiabatic processes and the Berry curvature in quantum mechanics [1]

An **adiabatic process** is one in which the external conditions of a system are changed gradually. In other words, if the system at hand has its own natural timescale, an adiabatic process is one in which the external conditions are changed much more slowly than this natural timescale. An extreme example of this is Earth's rotation around the sun. The natural timescale of our day to day lives is much, much faster than our change in position in the universe. As a result, whether or not I decide to take a nap, go to the grocery store, or exercise, has very little to do with what season it is (unless you live in some place with terrible weather!). To put this concept on more rigorous footing, if a particle is in the n^{th} eigenstate of some initial Hamiltonian, $\mathcal{H}_i$, then as an external change is made such that the new Hamiltonian becomes $\mathcal{H}_f$, the particle with remain in the n^{th} eigenstate of $\mathcal{H}_f$.

Now suppose that the external parameters are changed in a cyclical way such that $\mathcal{H}_i \to \mathcal{H}_f \to \mathcal{H}_f$. Quantum mechanics tells us that the particle's final state only needs to be the same as the initial state up to a relative phase factor. If this phase factor is nonzero, the system is said to be **nonholonomic** (Figure 1). To see this, we can take the Schrodinger equation:

$$\mathcal{H}\psi_n(x) = E_n\psi_n(x) \tag{1}$$

The state will evolve according to

$$\psi_n(x,t) = \psi_n(x,0)e^{-iE_nt/\hbar} \tag{2}$$

If the Hamiltonian changes adiabatically,

$$H(t)\psi_n(x,t) = E_n(t)\psi_n(x,t) \tag{3}$$

then

$$\psi_n(x,t) = \psi_n(x,0)e^{-iE_n\frac{t}{\hbar}}e^{-\frac{i}{\hbar}\int_0^t dt' E_n(t')}e^{-i\gamma_n(t)} \tag{4}$$

where the first part of the right hand side is the same as equation (2), the second phase factor is called the dynamic phase, and the third phase factor, $\gamma_n(t)$, is called the geometric phase.

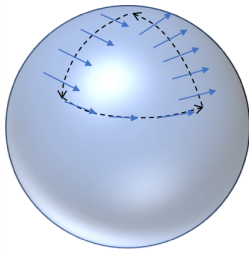

Figure 1: An arrow traveling around a closed path on a curved surface. When the arrow is returned to its starting position, it will be rotated by some nonvanishing angle, called the "Berry phase."

We would like to know what this geometric phase is. If we recall the differential form of the Schrodinger equation

$$i\hbar\frac{\partial\psi}{\partial t} = \mathcal{H}\psi \tag{5}$$

and plug in equation (4), we get an expression for $\gamma_n(t)$:

$$\dot{\gamma_n}(t) = i\hbar\langle\psi_n|\dot{\psi_n}\rangle \tag{6}$$

If R(t) is the external parameter that we change in time, then $\dot{\psi_n} = \frac{\partial\psi_n}{\partial R}\dot{R}$ and integrating equation (6) gives

$$\gamma_n(t) = i\int_{R_i}^{R_f} dR\,\langle\psi_n|\frac{\partial\psi_n}{\partial R}\rangle \tag{7}$$

Okay, now obviously if R_i=R_f, the geometric phase will be 0. Instead, if we allow for more than one external parameter to change:

$$\dot{\psi_n} = \frac{\partial\psi_n}{\partial R_1}\dot{R}_1 + \frac{\partial\psi_n}{\partial R_2}\dot{R}_2 + ... \tag{8}$$

$$= \nabla_{\mathbf{R}}\psi_n\cdot\dot{\mathbf{R}}^2 \tag{9}$$

And finally, we get the result for the **Berry phase**:

$$\boxed{\gamma_n(t) = i \oint \langle \psi_n | \nabla_{\mathbf{R}} \psi_n \rangle \cdot d\mathbf{R}} \tag{10}$$

The Berry phase must be real, path dependent, and yet independent of the elapsed time. This is in contrast to the dynamic phase, which clearly depends on the elapsed time.

It is often the case that people talk about the Berry phase in the context of a ficticious "magnetic field," called the Berry curvature. To see why this is, recall that the magnetic flux, Φ, through a surface S bounded by a closed curve C is

$$\Phi = \int_S \mathbf{B} \cdot d\mathbf{a} \tag{11}$$

$$= \int_S (\nabla \times \mathbf{A}) \cdot d\mathbf{a} \tag{12}$$

$$= \oint_C \mathbf{A} \cdot d\mathbf{r} \tag{13}$$

where the second equality comes from the relationsihp between a magnetic field **B** and its vector potential **A** and the third equality comes from Stokes theorem. Comparing the form of equation 13 with our equation for for the Berry phase (10), we see that i $\langle \psi_n | \nabla_{\mathbf{R}} \psi_n \rangle$ is like a vector potential with a corresponding "magnetic field"

$$\boxed{\Omega_n = i \nabla_{\mathbf{R}} \times \langle \psi_n | \nabla_{\mathbf{R}} \psi_n \rangle} \tag{14}$$

This magnetic field-like quantity is what we call the **Berry curvature**.

2 How does the Berry phase affect electronic motion in solids? [2]

First, we will ask what the equation of motion is for an electron in a periodic potential. We will find that the inclusion of a slowly varying static potential in our solid, akin to a lattice, requires us to modify our equation of motion by adding the effects of a Berry curvature. In the end, we will find that the Berry curvature can be nonzero and significantly affect electronic motion in crystals with broken inversion and/or time-reversal symmetry.

To begin, we must come up with an equation of motion for an electron in an effective potential. We will remain under the assumption that an electron in band n cannot evolve into any other band m≠n. Ehrenfest's theorem tells us that the velocity **v** of an electron in a lattice is

$$\mathbf{v} = \frac{d\mathbf{R}}{dt} = \frac{\partial \mathbf{R}}{\partial t} \frac{1}{i\hbar} [\mathbf{R}, \mathcal{H}_{\text{eff}}] \tag{15}$$

$$= \frac{1}{\hbar} \nabla_{\mathbf{k}} E_n(\mathbf{k}) \tag{16}$$

and Bloch's theorem tells us that its wavefunction is

$$\langle r | n\mathbf{k} \rangle = \psi_{n\mathbf{k}} = e^{i\mathbf{k}\cdot\mathbf{r}} u_{n\mathbf{k}}(\mathbf{r}) \tag{17}$$

However, in a static, but slowly varying external potential, we should expect the electron to drift in k-space. According to the adiabatic approximation, as the electron moves though k-space, it can pick up both an additional dynamic phase factor and an additional geometric phase factor, the latter of which we can call γ_n. The slowly varying external potential should remind us of the gradually changing external parameter discussed in the previous section. In analogy to equations (10) and (14), we can match terms to write down the Berry phase and Berry curvature.

$$\Omega_n = i \nabla_{\mathbf{k}} \times \langle u_{n\mathbf{k}} | \nabla_{\mathbf{k}} u_{n\mathbf{k}} \rangle \tag{18}$$

$$= \nabla_{\mathbf{k}} \times A_n \tag{19}$$

$$\gamma_n = \oint d\mathbf{k} \cdot A_n \tag{20}$$

Now, what I'd like to show is that the Berry curvature is an intrinsic part of the band structure that will affect an electronic motion. If you recall $\mathcal{H} = E_n\mathbf{k} + U(R)$ where R=i$\nabla_{\mathbf{k}}$. We just showed that the motion of an electron in this Hamiltonian will give rise to a Berry phase that we must account for. We are free to perform a gauge transformation to remove the geometric phase from the Bloch wavefunction of the form of equation (4). If we do this, then

$$\mathcal{H} \to \mathcal{H}' = E_n\mathbf{k} + U(R + A_n(\mathbf{k})) \tag{21}$$

Redefining $\mathbf{x} = R + A_n(\mathbf{k})$, it can be shown that the components of **x** do not commute with one another. More specifically:

$$[x_i, x_j] = i\epsilon^{ijk} \Omega_n(\mathbf{k}) \tag{22}$$

and our equation of motion (16) must be modified to include an additional term:

$$\mathbf{v} = \frac{1}{\hbar} \nabla_{\mathbf{k}} E_n(\mathbf{k}) + \frac{1}{\hbar} \nabla_{\mathbf{x}} \times \Omega_n(\mathbf{k}) \tag{23}$$

This added term on the right hand side is called the Luttinger, or anomalous velocity.

You might be wondering...why do people often neglect the Berry curvature if it so clearly enters into an

electron's equation of motion. Any crystal that possesses both time-reversal (v→-v, k→-k, E→E) and inversion symmetry (v→-v, k→-k, E→-E) must necessarily have a vanishing Berry curvature. One can see this by plugging in these symmetries to equation (23) and noting that for a crystal with time-reversal symmetry $\Omega_n(-\mathbf{k}) = -\Omega_n(\mathbf{k})$ whereas for a crystal with inversion symmetry $\Omega_n(-\mathbf{k}) = \Omega_n(\mathbf{k})$. For both of these statements to be true, $\Omega_n(\mathbf{k}) = 0$. It should be noted that this arguement breaks down at degenerate points in k-space where electrons can travel between two bands (which I'm assuming is why the anomolous Hall effect is observed in Weyl semimentals but I'm not sure about this one).

3 The Band Structure of MoS_2 [3]

MoS_2 is a group-IV transition metal dichalgogenide TMDC of the form MX_2. Bulk TMDC materials are often exfoliable as 2D materials since the van der Waals forces that dominate the interlayer coupling are relatively weak. In monolayer MSo_2, the conduction band (CB) and valence band (VB) edges are located at the K and K' points of a 2D hexagonal Brillouin zone (Figure 2). While the same is true for many other relevant 2D materials, like graphene, monolayer MoS_2 has two unique properties:

1. It has broken inversion symmetry.
2. The 4d orbitals of Mo have strong spin orbit coupling (SOC).

We will soon see that combination of these two intrinsic properties gives rise to coupled spin and valley degrees of freedom at the root of MoS_2's interesting optical and electronic properties.

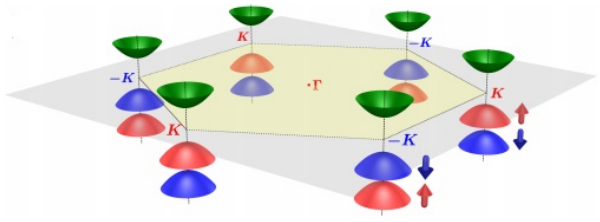

Figure 2: The Brillouin zone in MoS_2. The K and -K (K') points at the Brillouin zone edges are connected by time-reversal symmetry. We note gaps between the valence and conduction bands that are opened at the K and -K points. We also note the splitting in the valence band that separates spin-down and spin-up electrons at the K and K' points. [3]

Let's first consider what the band structure of MoS_2 may look like. Given the d-character of the Mo valence electrons, we should expect bands near the Fermi level to be d-like. The trigonal prismatic coordination environment of the Mo atoms also serves to split its d-orbitals into three groups: $A_1(d_{z^2}), E(d_{xy}, d_{x^2-y^2}), E'(d_{xz}, d_{yz})$. In the monolayer limit, the presence of an xy mirror plane allows only for A_1 and E orbitals to hybridize with one another, thus opening up gaps at the K and K' points. If that conclusion doesn't make sense, recall from your introductory chemistry course that when two atomic orbitals hybridize, they form two bonding and anti-bonding orbitals separated by a gap. The gap at the K and K' points can be thought of as arising in a similar manner. We can approximate the wavefunctions in the VB and CB using a linear combination of atomic orbitals (LCAO) approach:

$$|\phi_{\mathrm{CB}}\rangle = |d_{z^2}\rangle \tag{24}$$

$$|\phi^{\tau}_{\mathrm{VB}}\rangle = \frac{1}{\sqrt{2}}(|d_{x^2-y^2}\rangle + i\tau\,|d_{xy}\rangle) \tag{25}$$

where $\tau = \pm 1$ is the valley index and $|\phi^{\pm 1}_{\mathrm{VB}}\rangle$ are related by time-reversal symmetry. Now, we can use these wavefunctions to approximate the Hamiltonian $\mathcal{H}_0$ at the K and K' points using $k\cdot p$ perturbation theory. This is a perturbation theory method commonly used in solid state physics to calculate the band structure around a particular point in k-space. What we end up with is:

$$\mathcal{H}_0 = at(\tau k_x \hat{\sigma}_x + \tau k_y \hat{\sigma}_y) + \frac{\Delta}{2}\hat{\sigma}_x \tag{26}$$

where $\hat{\sigma}_\alpha$ are the Pauli matrices for the two basis functions and a, t, and Δ are the lattice constant, hopping term, and band gap, respectively, that are all tabulated constants. Now this Hamiltonian didn't include SOC, which we know we should include given the strong SOC present in Mo. If you recall, SOC is nothing but an extra term in the Hamltonian of the form $L \cdot S$ where L and S are the orbital and spin angular momentum operators, respectively. Including this term in our Hamiltonian gives rise to an updated Hamiltonian in the VB of the form:

$$\boxed{\mathcal{H} = \mathcal{H}_0 - \lambda\tau\frac{\hat{\sigma}_z - 1}{2}\hat{s}_z} \tag{27}$$

where 2λ is the spin splitting at the valence band top due to the SOC and $\hat{s}_z$ is the Pauli matrix for a spin-1/2 particle:

$$\hat{s}_z\,|\uparrow\rangle = |\uparrow\rangle \tag{28}$$

$$\hat{s}_z\,|\downarrow\rangle = -\,|\downarrow\rangle \tag{29}$$

We see that the valence band is split due to SOC and that τ enters here. Time-reversal symmetry thus dictates that the spin-splitting in the VB must be opposite

at the K and K' points (Figure 2). We will now explore the effects of this spin-valley coupled band structure observable as electronic and optical properties.

3.1 Electronic properties of MoS_2

We learn in introductory solid state physics about the Hall effect, namely, when an in plane electric field is applied in combination with a transverse magnetic field, a Hall current will result in the third orthogonal direction (Figure 3).

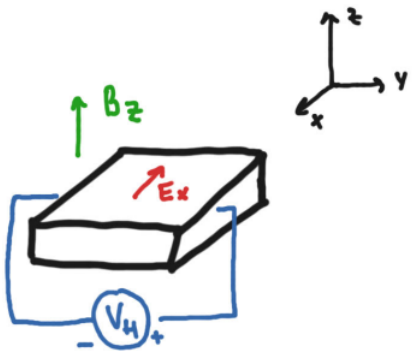

Figure 3: The Hall effect

We recall from section 1 that the Berry curvature looks a lot like a magnetic field. The anomalous Hall effect can be observed in materials with a large Berry curvature without an external magnetic field. In other words, with the application of an in-plane electric field, electrons will acquire an in-plane, but transverse velocity proportional to the Berry curvature in the out of plane direction. Mathematically, we can describe the conductivity resulting from this anomalous hall effect as

$$\sigma = \frac{e^2}{\hbar}\int \frac{dk}{(2\pi)^2} f(k)\Omega_{z,n}(k) \tag{30}$$

where f(k) is the Fermi-Dirac distribution and $\Omega_{z,n}(k)$ is the z-projection of the Berry curvature we wrote down in equation (14):

$$\Omega_{z,n}(k) = \hat{z}\cdot i\nabla_{\mathbf{k}} \times \langle u_{n\mathbf{k}}|\nabla_{\mathbf{k}} u_{n\mathbf{k}}\rangle \tag{31}$$

Using our Hamiltonian in equation (27) to get the Bloch states, $|u_{nk}\rangle$ and plugging them into equation (31), we arrive at the Berry curvatures in the CB and VB:

$$\Omega_{\mathrm{CB}}(k) = -\tau\frac{2a^2t^2\Delta'}{[\Delta'^2 + 4a^2t^2k^2]^{\frac{3}{2}}} \tag{32}$$

$$\Omega_{\mathrm{VB}}(k) = -\Omega_{\mathrm{CB}}(k) \tag{33}$$

where $\Delta' = \Delta - \tau\hat{s}_z\lambda$. Here, we should notice two key things:

1. With the presence of τ, the Berry curvature has opposite signs in the different K and K' valleys.
2. The appearence of λ in the Δ' term means that the Berry curvature is dependent on the spin-splitting in the valence band.

Now we can input equations (32) and (33) back into equation (30) as we'd like to get the spin and valley anomalous hall conductivities:

$$\sigma^n_{\mathrm{valley}}(k) = 2\int \frac{dk}{(2\pi)^2}[f_{n\uparrow}(k)\Omega_{n\uparrow}(k) + f_{n\downarrow}(k)\Omega_{n\downarrow}(k)] \tag{34}$$

$$\sigma^n_{\mathrm{spin}}(k) = 2\int \frac{dk}{(2\pi)^2}[f_{n\uparrow}(k)\Omega_{n\uparrow}(k) - f_{n\downarrow}(k)\Omega_{n\downarrow}(k)] \tag{35}$$

where the integration is performed about a single K point. The valley- and spin-Hall conductivites are quite robust because the valley and spin are good quantum numbers. In other words, the valley and spin quantum numbers must be flipped simultaneously if they are to be flipped at all. To flip the former requires an atomic-scale scatterer since K and K' are the size of the Brillouin zone apart, whereas to flip the latter requires a magnetic scatterer. Therefore, without the presence of large, atomic-scale magnetic scattering centers, we should expect the conductivities of equations (34) and (35) to be persistant.

3.2 Optical Properties of MoS_2

The interband matrix element for optical transitions across a band gap is given by:

$$\mathcal{P}_\alpha(k) = m_o\langle u_{\mathrm{CB}}|\frac{1}{\hbar}\frac{\partial\mathcal{H}}{\partial k_\alpha}u_{\mathrm{VB}}\rangle \tag{36}$$

where $\alpha \in \{x, y, z\}$ and the coupling strength is proportional to this matrix element. For circularly polarized light which we'll denote with indices of $\pm$, $\mathcal{P}_\pm(k) = \mathcal{P}_x \pm i\mathcal{P}_y$. Using $\mathcal{H}$ from equation (27), we can evaluate the matrix elements for coupling to circularly polarized light explicitly:

$$|\mathcal{P}_\pm(k)|^2 = \frac{m_o^2a^2t^2}{\hbar^2}\left[1 \pm \tau\frac{\Delta'}{\sqrt{\Delta'^2 + 4a^2t^2k^2}}\right]^2 \tag{37}$$

Here, we see that circularly-polarized light is coupled differently to the K and K' valleys with $\tau = \pm 1$. We note that light cannot flip spins, so we also can conclude that circularly polarized light incident on MoS_2 will couple with spin selectivity. If we return to our Hamiltonian of equation (27), we recall that the spin gap in the valence

band is flipped at the K and K' points. For example, at the K point, the $|\uparrow\rangle$ band is higher in energy than the $|\downarrow\rangle$ band, while the opposite is true at the K' point. The net result is that by tuning the helicity of light and its wavelength, one has complete control over spin and valley degrees of freedom (Figure 4). It is then possible to imagine separating carriers of different types in a Hall bar geometry because of the opposing directions electrons and holes will travel due to their oppositely signed Berry curvature. A set of experimental schemes of this sort are described in [3].

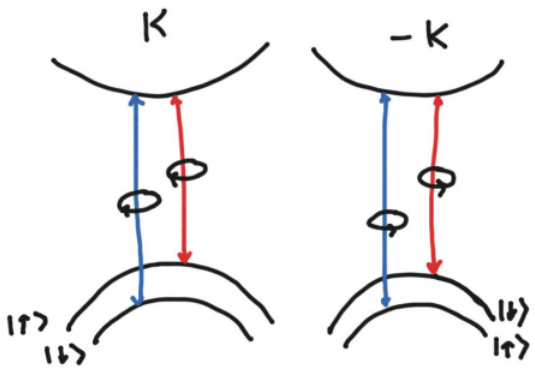

Figure 4: By tuning the wavelength and polarization of light, one has complete optical control over the spin and valley quantum number of carriers.

References

[1] David J. Griffiths and Darrell F. Schroeter. *Introduction to Quantum Mechanics*. Cambridge University Press, aug 2018.

[2] Marvin Cohen and Steven Louie. *Fundamentals of Condensed Matter Physics*. Cambridge University Press, 1st edition, 2016.

[3] Di Xiao, Gui-Bin Liu, Wanxiang Feng, Xiaodong Xu, and Wang Yao. Coupled Spin and Valley Physics in Monolayers of MoS2 and Other Group-VI Dichalcogenides. *Phys. Rev. Lett.*, 108(19):196802, may 2012.